JOURNAL OF APPLIED ELECTROCHEMISTRY 27 (1997) 71–75

Ionic conductivity of perovskite $LaCoO_3$ measured by oxygen permeation technique

C. H. CHEN*, H. KRUIDHOF, H. J. M. BOUWMEESTER, A. J. BURGGRAAF

Laboratory for Inorganic Chemistry, Materials Science and Catalysis, Faculty of Chemical Technology, University of Twente, 7500 AE Enschede, The Netherlands

Received 26 March 1996; revised 29 April 1996

Oxygen permeation measurement is demonstrated, not only for a mixed oxide ionic and electronic conductor, but also as a new alternative to determine ambipolar conductivities, which can be usually reduced to be partial conductivities (either ionic or electronic). As a model system and an end member of an important oxygen permeable $La_{1-x}Sr_xCoO_{3-\delta}$ dense membrane system, $LaCoO_3$ dense ceramic was measured with respect to the thickness, temperature and oxygen partial pressure dependencies of its oxygen permeability. Within the thickness range used (down to 0.041 cm), the oxygen permeation of $LaCoO_3$ was found to be purely controlled by bulk diffusion with activation energies between 260–300 kJ mol^{-1}. Its ionic conductivity and oxygen self-diffusion coefficient as functions of oxygen partial pressure were also derived from permeability data. $P_{O_2}^{-0.46}$ and $P_{O_2}^{-0.31}$ relations were found in the high pressure (1.01–10^{-2} bar) and low pressure ($10^{-2.8}$–$10^{-3.4}$ bar) ranges, respectively.

1. Introduction

Mixed ionically and electronically conducting oxides are important electrode materials in electrochemical devices such as solid oxide fuel cells (SOFCs) and gas sensors. They are also under intensive investigation for use as chemical reactors and gas separation membranes. The most critical characteristics of these type of materials are their electrical conductivities, including total conductivity (σ_{total}), ionic conductivity (σ_{ion}) and electronic conductivity (σ_{el}). Traditionally, σ_{total} can be easily measured by either direct current (d.c.) (e.g., d.c. four-probe method) or alternating current (a.c.) (e.g., complex impedance spectroscopy) methods. However, the partial conductivities, σ_{ion} and σ_{el}, can only be deconvoluted from σ_{total} with additional measurement by other means. One method is measuring the transference number (t_{ion} or t_{el}) by a concentration difference cell [1, 2]. This is usually suitable when t_{ion} and t_{el} are comparable. If σ_{el} is much larger than σ_{ion}, as in the case of perovskite mixed conductors, a too small electric potential difference makes it difficult to obtain accurate σ_{ion} values. Another method is using an electrode to block the transport of one kind of charge carrier and thus measure the conductivity of the other [3]. For a predominantly electronically conducting material, an electron-blocking electrode such as yttria-stabilized zirconia (YSZ) may be used. When σ_{ion} of a mixed conductor is considerably higher than that of the blocking electrode, a four-probe measurement may be necessary [4, 5]. However, there are also some difficulties with this method, such as chemical interaction between the blocking electrode and the mixed conductor at elevated temperatures [6] and gas leakage problems. In addition to the above-mentioned two methods, σ_{ion} can also be obtained through measuring oxygen diffusivity [7].

In general, direct measurement of partial conductivity of the minority charge carrier of a mixed conductor is difficult by conventional techniques. Recently, Riess used a 'zero driving force' method to measure the ionic conductivity of a mixed conductor [8, 9]. By externally short circuiting a mixed conductor subjected to an oxygen gradient, its ionic conductivity can be derived from the current caused by ionic conduction. Nevertheless, this method is especially suitable for measurement of a P_{O_2}-independent oxygen ionic conductivity. Otherwise, only an average conductivity is obtained. On the other hand, Patrakeev *et al.* adopted an oxygen permeation technique and successfully measured the oxygen partial pressure dependence of the oxygen ionic conductivity of $YBa_2Cu_3O_{6+\delta}$ [10]. The measurement was performed under a small P_{O_2}-gradient.

In this study we used, for the first time, an appropriate procedure for oxygen permeation measurement and data treatment to derive the oxygen partial pressure dependence of the ambipolar conductivity of $LaCoO_3$, which is an end member of the highly oxygen permeable $La_{1-x}Sr_xCoO_{3-\delta}$ system. In this particular case, the ambipolar conductivity is approximately the ionic conductivity of $LaCoO_3$. This method is analogous to the method suggested by Wagner in his investigation of metal oxidation [11].

* To whom correspondence should be addressed at Laboratory for Applied Inorganic Chemistry, Delft University of Technology, Julianalaan 136, 2628 BL Delft, The Netherlands.

0021-891X

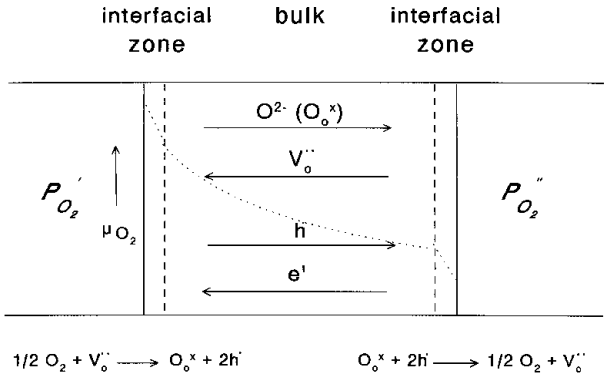

Fig. 1. A scheme of oxygen permeation through a dense membrane.

2. Theory

The scheme of oxygen permeation through a mixed conductor dense membrane is shown in Fig. 1, where the oxygen partial pressure at the gas feed side, P'_{O_2}, is larger than that at the permeate side, P''_{O_2}. The membrane can be divided into three zones in the permeation direction, that is, two interfacial zones at surfaces and an intermediate bulk zone. The transport directions of related charged species are also shown in the figure. If the permeation is a volume diffusion rate-limited, one-dimensional and steady state process, an integral form of Wagner's equation can be applied to calculate oxygen permeability:

$$j_{O_2} = -\frac{RT}{4^2F^2L}\int_{\ln P'}^{\ln P''} \frac{\sigma_{ion}\sigma_{el}}{\sigma_{total}}\, d\ln P \qquad (1)$$

where, σ_{ion}, σ_{el} and σ_{total} are the ionic conductivity, the electronic conductivity and the total conductivity of the membrane, respectively. R is the gas constant, F the Faraday constant, and L the membrane thickness. The integrated term $\sigma_{ion}\sigma_{el}/\sigma_{total}$ is defined as the ambipolar conductivity σ_{amb} of the membrane, which is generally a function of oxygen partial pressure. It may also be written as

$$\sigma_{amb} = \frac{\sigma_{ion}\sigma_{el}}{\sigma_{ion}+\sigma_{el}} = \frac{\sigma_{ion}\sigma_{el}}{\sigma_{total}} = t_{ion}\sigma_{el} = t_{el}\sigma_{ion} = t_{ion}t_{el}\sigma_{total} \qquad (2)$$

Therefore,

$$j_{O_2} = \frac{RT}{4^2F^2L}\int_{\ln P''}^{\ln P'} \sigma_{amb}(P)\, d\ln P \qquad (3)$$

If the oxygen partial pressure at one side, for instance P', is fixed, measuring the isothermal oxygen permeability j_{O_2} as a function of P'', then $\sigma_{amb}(P'')$ can be obtained by

$$\sigma_{amb}(P'') = -\frac{4^2F^2L}{RT}\left[\frac{\partial j_{O_2}}{\partial \ln P''}\right]_{P'=\text{constant}} \qquad (4)$$

Similarly, $\sigma_{amb}(P')$ can be obtained by fixing P'' and varying P'.

It should be emphasized again that Equations 1, 3 and 4 hold only if the total oxygen transport is predominantly controlled by the bulk volume diffusion process. This is, in principle, always true when the membrane is thick enough and the diffusion along grain boundaries are negligible. In practice, however, the thickness of a mixed conductor can not be increased indefinitely. Therefore, the first step is to ensure that the thickness of the membrane satisfies the condition of the bulk diffusion control. This can be done by checking the thickness dependence of the oxygen permeability.

3. Experimental details

3.1. *Preparation of dense compacts of $LaCoO_3$*

AR grade $La(NO_3)_3\cdot 6H_2O$ and $Co(NO_3)_3\cdot 6H_2O$ were weighed in a 1 : 1 molar ratio and dissolved in a small amount of distilled water (solution 1). In a slurry of EDTA (Titriplex II) in water, ammonia was added until the EDTA was dissolved completely. The amount of EDTA was taken in the ratio of 3 mole EDTA per mole $LaCoO_3$. After the EDTA was dissolved, the pH was adjusted to about 8.5 (solution 2). Solution 2 was added to solution 1, and the final solution was adjusted to a pH of 8–9. The solution was stirred on a hot plate until it became rather viscous. It was then transferred to a beaker and evaporated in a furnace at 250 °C. During the evaporation a foam developed on top of the solution. Upon further heating this foam pyrolysed into a fine powder.

The powder was calcined at 900 °C for 16 h in air and then was ball milled for 2 h. It was then pressed uniaxially at 170 kPa, and then isostatically pressed at 400 MPa. The density of the obtained green compacts was 54% of the theoretical density of $LaCoO_3$. The compacts were sintered in air at 1150 °C for 10 h with heating and cooling rates of 1.5 °C min^{-1}. Finally, completely crack-free $LaCoO_3$ discs with relative densities of about 98% were obtained. These were identified by XRD as of perovskite structure. The discs were cut and polished on a 1000 mesh sand paper to final sizes of 1.5 cm in diameter and thicknesses from 0.041 cm to 0.233 cm for oxygen permeation.

3.2. *Oxygen permeation measurement*

The oxygen permeation of four sintered $LaCoO_3$ discs with different thicknesses (0.041, 0.098, 0.16 and 0.233 cm, respectively) were measured in the temperature range 1000–1100 °C. The setup and working principle have been described elsewhere [12]. In this study, Supremax glass rings (Schott, Nederland BV), instead of Duran, were used to seal the discs into the reactor. To be close to one-dimensional diffusion, the side walls of the specimens were coated with fine Duran glass powder by painting and *in situ* heating. An oxygen/nitrogen gas mixture was fed to one side (60 ml min^{-1}), while the other side was flushed with high purity helium gas ($P_{O_2} = 4\times10^{-5}$ bar) at controlled flow rates (5–50 ml min^{-1}). Oxygen concentration and the amount of oxygen permeating

through a specimen were determined by online gas chromatography (Varian model 3400) at the gas outlet of permeate side. In the mean time, the oxygen partial pressures at gas outlets for both sides were monitored by oxygen gas sensors working at 700 °C. The oxygen partial pressure P_{O_2} at the feed side was controlled by changing the flow rate ratio f_{O_2}/f_{N_2} ($f_{O_2}+f_{N_2}=60\,\mathrm{ml\,min^{-1}}$), while P_{O_2} at the permeate side was controlled by varying the helium sweep rate. If a constant-stirring-tank-reactor (CSTR) condition could be achieved, the P_{O_2} at the gas outlets were equal to those on the surfaces of the specimen. According to studies performed in our laboratory, the CSTR condition seems to hold under our measurement conditions. Based on a numerical solution of non-one-dimensional diffusion, corrections were made for oxygen permeability data deviation caused by the sealing, and thus the different active surface areas on the two sides of the discs [13].

4. Results and discussion

The temperature dependencies of the oxygen permeation of three $LaCoO_3$ specimens with different thicknesses are shown in Fig. 2. It can be seen that, owing to small oxygen vacancy concentration in $LaCoO_3$, its oxygen permeability is about one order of magnitude lower than that of strontium-doped $LaCoO_3$ [14]. The activation energies are from $260\,\mathrm{kJ\,mol^{-1}}$ to $300\,\mathrm{kJ\,mol^{-1}}$. They are very close to reported activation energies of oxygen tracer diffusion coefficients for $LaCoO_3$ [15], suggesting that the rate limiting step for the oxygen permeation is bulk diffusion. Although the activation energy seems to increase with increasing thickness, a definite correlation between them can not be derived here due to the small measurement temperature range (i.e., 1000–1100 °C) in this study and, hence, the relatively large errors in the derived activation energy values.

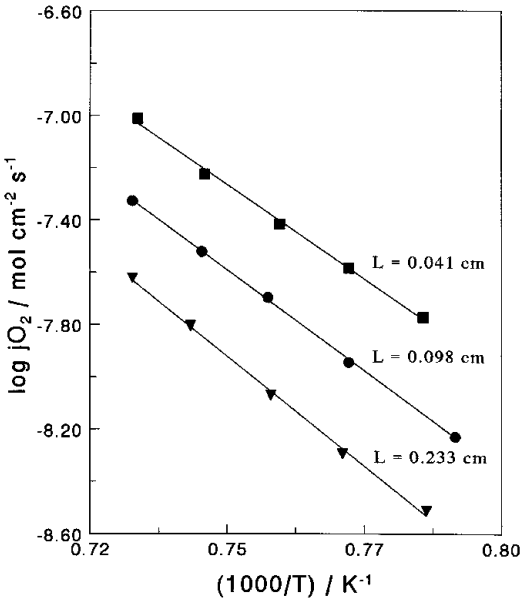

Fig. 2. The temperature dependence of the oxygen permeation of $LaCoO_3$. Thickness and P'–P'': (■) 0.041 cm, 0.21–0.0040 bar; (●) 0.098 cm, 0.21–0.0017 bar; (▼) 0.233 cm, 0.21–0.0011 bar.

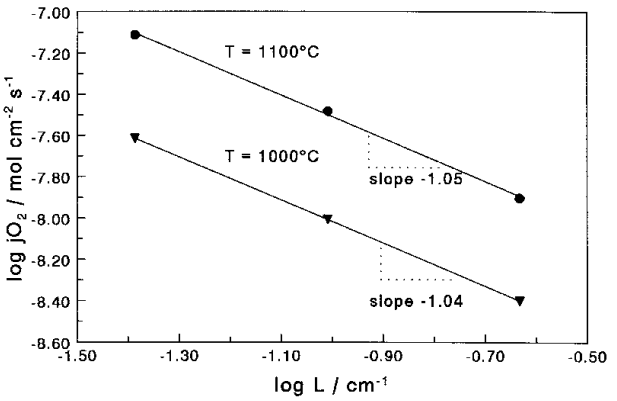

Fig. 3. The thickness dependence of the oxygen permeation of $LaCoO_3$. Temperature and P'–P'': (●) 1100 °C, 0.21–0.0069 bar; (▼) 1000 °C, 0.21–0.000 81 bar.

The most convincing evidence concerning the rate limiting step for the oxygen permeation comes from the permeability-thickness relationship. Figure 3 shows the thickness dependencies of the oxygen permeation of $LaCoO_3$ at 1000 °C and 1100 °C under fixed oxygen partial pressures at both sides. The two lines of the $\log j_{O_2} - \log L$ relation have slopes of −1.05 and −1.04. Considering experimental errors, for instance, the error in measuring the surface areas or the incomplete coverage of side walls by glass powders, the slopes derived here indicate an exactly inverse proportionality relation between the oxygen permeability (j_{O_2}) and the thickness (L) of the $LaCoO_3$ membrane. Therefore, the oxygen permeation of $LaCoO_3$ membranes thicker than 0.041 cm must be purely controlled by bulk diffusion. This confirms the conclusion obtained from the activation energy, and guarantees the validity of calculating the ambipolar conductivity of $LaCoO_3$ by Equation 4 thereafter, as long as the $LaCoO_3$ membrane thickness is greater than 0.041 cm.

Figure 4 shows relations between the oxygen permeability of a 0.16 cm thick $LaCoO_3$ disc and the oxygen partial pressures at the feed side (P') (Fig. 4(a)) and permeate side (P'') (Fig. 4(b)). By polynomial fitting (order 3 for P' dependence, order 2 for P'' dependence), smooth j_{O_2}–$\log P$ relation curves were drawn as shown. From local slopes of the curves, the ambipolar conductivity ($\sigma_{amb} = t_i \sigma_{el}$) at an oxygen partial pressure may be calculated according to Equation 4. It is found that the order of magnitude for σ_{amb} at 900 °C is $10^{-3}\,\mathrm{S\,cm^{-1}}$. Since the electronic conductivity (σ_{el}) of $LaCoO_3$ at 1000 °C is as high as $10^{3}\,\mathrm{S\,cm^{-1}}$ [16], its ionic transference number t_{ion} should be much less than unity and the derived ambipolar conductivity of $LaCoO_3$ must be equal to its ionic conductivity. The conductivity calculation results are shown in Fig. 5. It can be seen that the ionic conductivity of $LaCoO_3$ decreases with increasing oxygen partial pressure. Obviously, this is due to the fact that the oxygen ionic conduction of $LaCoO_3$ proceeds through a vacancy mechanism and an increase in oxygen partial pressure lowers the

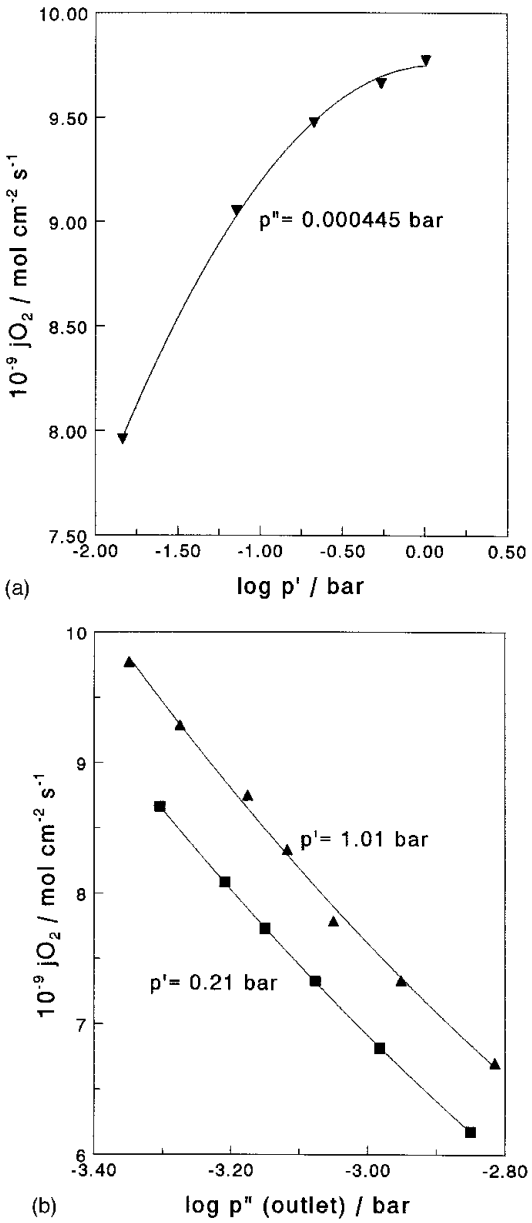

Fig. 4. The oxygen partial pressure dependence of the oxygen permeation of a 0.16 cm thick $LaCoO_3$ membrane at 1000 °C, (a) high pressure (P') dependence; (b) low pressure (P'') dependence. The fixed pressures are given in figures.

oxygen vacancy concentration in $LaCoO_3$. Unlike aliovalent element doped $LaCoO_3$ such as $La_{0.4}Sr_{0.6}CoO_{3-\delta}$, where the oxygen vacancy concentration is mainly determined by doping level, the oxygen vacancy concentration in the undoped material depends strongly on the oxygen partial in the ambient. It is also noted that the low pressure (P'') dependencies (Fig. 4(b)) measured under two fixed high pressures ($P' = 1.01$ bar and $P' = 0.21$ bar) gives rise to almost identical conductivity values. This reflects a good accuracy of this method. A smooth ionic conductivity–log$P$ curve can be drawn by a polynomial fitting in the whole measurement partial pressure range ($10^{-3.4}$–1.01 bar) and can be described by

$$\sigma_{\text{ion}}P = (2.904 - 3.495\log P + 1.770\log^2 P - 0.807\log^3 P) \times 10^{-4}\,\text{S cm}^{-1} \quad (5)$$

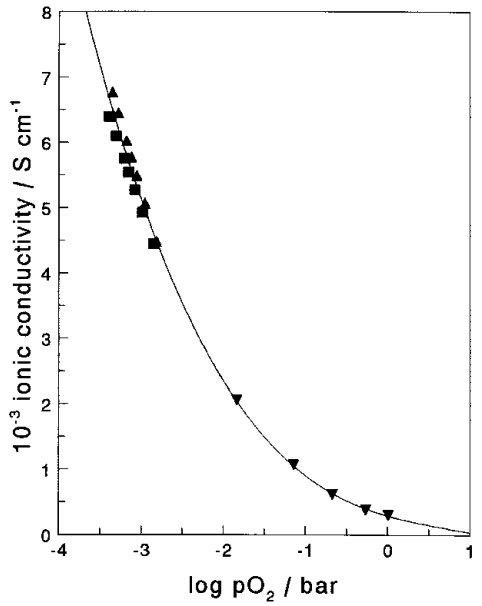

Fig. 5. The oxygen partial pressure dependence of the ionic conductivity of $LaCoO_3$ at 1000 °C calculated according to Equation 4. Marks (▲) and (■) represent the results from low pressure dependence while $P' = 1.01$ bar and $P' = 0.21$ bar, respectively, while (▼) represents results from high pressure dependence when $P'' = 0.000\,445$ bar.

According to the Nernst–Einstein relationship, the oxygen self-diffusion coefficient D_O in $LaCoO_3$ can also be calculated from its oxygen ionic conductivity. A double logarithmic figure of the ionic conductivity and the oxygen self-diffusion coefficient as functions of oxygen partial pressure is plotted in Fig. 6. Therefore, a power pressure dependence relation (i.e., σ_{ion} (or D_O) $\propto P_{O_2}^{-0.46}$) is obtained in the pressure range 1–10^{-2} bar. This agrees well with the pressure dependence of the nonstoichiometry of $LaCoO_3$($\delta \propto P_{O_2}^{-0.5}$) obtained from thermogravimetric measurement [17] and a coulometric titration method [18]. This implies

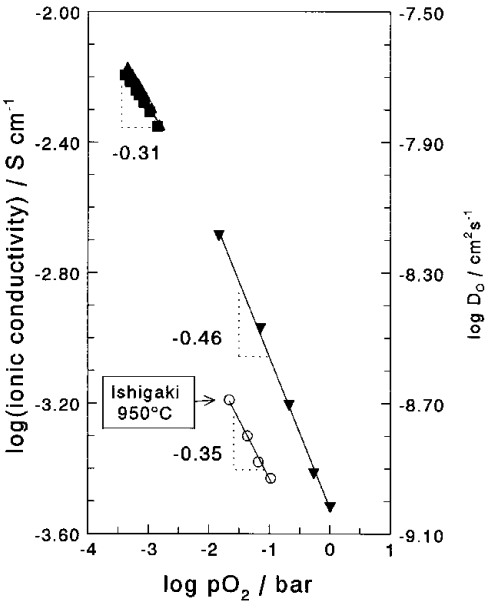

Fig. 6. Double logarithmic relations of logσ_{ion}–logP_{O_2} and logD_O–logP_{O_2} relation of $LaCoO_3$ at 1000 °C. Marks (▲) and (■) represent the results from low pressure dependence while $P' = 1.01$ bar and $P' = 0.21$ bar, respectively. Mark (▼) represents results from high pressure dependence when $P'' = 0.000\,445$ bar.

that all oxygen vacancies are fully ionized and dominate the oxygen ion transport. In addition, the order of magnitude of D_O is in a good agreement with that obtained by gas–solid isotopic exchange technique for single crystal $LaCoO_3$ [15], meaning that diffusion, not through grain boundaries, but through grain bulk plays a predominant role. The pressure dependence may be explained by the point defect equilibria in this system. Electrical conductivity and Seebeck coefficient measurements [19, 20] showed the metallic electrical properties of $LaCoO_3$. This is caused, especially at high temperatures, by a nearly complete charge disproportionation of Co(III):

$$2Co_{Co}^{\times} \rightleftharpoons Co_{Co}^{/} + Co_{Co}^{\cdot} \quad (6)$$

Thus,

$$K_{Co} = \frac{[Co_{Co}^{/}][Co_{Co}^{\cdot}]}{[Co_{Co}^{\times}]^2} \quad (7)$$

where K_{Co} is the equilibrium constant of Equation 6 which is independent of P_{O_2}. An oxygen atom may incorporate two electrons from two Co^{2+} and an oxygen vacancy site:

$$\tfrac{1}{2}O_2 + 2Co_{Co}^{/} + V_O^{\cdot\cdot} \rightleftharpoons O_O^{\times} + 2Co_{Co}^{\times} \quad (8)$$

The mass action law gives

$$K_V = \frac{[O_O^{\times}][Co_{Co}^{\times}]^2}{[V_O^{\cdot\cdot}][Co_{Co}^{/}]^2 P_{O_2}^{1/2}} = \frac{(3 - [V_O^{\cdot\cdot}])[Co_{Co}^{\times}]^2}{[V_O^{\cdot\cdot}][Co_{Co}^{/}]^2 P_{O_2}^{1/2}} \quad (9)$$

where K_V is the equilibrium constant, which is also independent of P_{O_2}. Since the oxygen vacancy concentration $[V_O^{\cdot\cdot}]$ in $LaCoO_3$ is very small, the $[Co^{2+}]$ consumed in Equation 8 must be very small. Also, $3 - [V_O^{\cdot\cdot}] \approx 3$ should hold. This means that $[Co_{Co}^{\cdot}] \approx [Co_{Co}^{/}]$, and Equation 9 can be reduced to

$$K_V \approx \frac{3}{[V_O^{\cdot\cdot}] P_{O_2}^{1/2} K_{Co}} \quad (10)$$

Therefore, from Equation 10, relations $[V_O^{\cdot\cdot}] \propto P_{O_2}^{-1/2}$ and σ_{ion} (or D_O) $\propto P_{O_2}^{-1/2}$ can be easily derived.

In the oxygen partial pressure range $10^{-2.8}$–$10^{-3.4}$ bar, Fig. 6 gives a relation σ_{ion} (or D_O) $\propto P_{O_2}^{-0.31}$. This is in agreement with the results from oxygen tracer diffusion coefficient measurements. Ishigaki reported a pressure dependence of the tracer diffusion coefficient of $LaCoO_3$ at 950 °C that D_O^* is proportional to $P_{O_2}^{-(0.35 \pm 0.04)}$ [15]. Furthermore, a study of nonstoichiometry in $LaCoO_3$ also supported a levelling-off trend of $\log(\sigma_{ion})$ in the low pressure range [17]. However, the mechanism behind the deviation from $P_{O_2}^{-1/2}$ dependence is not yet clear.

5. Conclusions

The oxygen partial pressure dependence of the ambipolar conductivity of a mixed conductor can be obtained by means of oxygen permeation measurement with appropriate measurement procedures. The oxygen permeation of dense $LaCoO_3$ membranes thicker than 0.041 cm is controlled by bulk diffusion. The power pressure dependencies of the ionic conductivity and oxygen self-diffusion coefficient for $LaCoO_3$ are σ_{ion} (or D_O) $\propto P_{O_2}^{-0.46}$ in the oxygen partial pressure range 1–10^{-2} bar, and σ_{ion} (D_O) $\propto P_{O_2}^{-0.31}$ in the pressure range $10^{-2.8}$–$10^{-3.4}$ bar.

Acknowledgements

This study was performed under a collaboration programme between the Academia Sinica and the Dutch Academy of Sciences (KNAW) and financially supported by the latter. Professor Meng Guangyao (Department of Materials Science and Engineering, University of Science and Technology of China) is gratefully acknowledged for stimulating this project. We are also indebted to Dr B. A. van Hassel and Dr Chen Chu-sheng for helpful discussions.

References

[1] C. Wagner, *in* 'Advanced Electrochemical Engineering', vol. 4 (edited by P. Delahay), Wiley, New York, (1966) p. 40.
[2] H. L. Tuller, *in* 'Nonstoichiometric Oxides' (edited by O. T. Sørensen), Academic Press, New York (1981) p. 271.
[3] M. H. Hebb, *J. Chem. Phys.* **20** (1952) 185.
[4] Y. Teraoka, H. M. Zhang, K. Okamoto and N. Yamazoe, *Mat. Res. Bull.* **23** (1988) 51.
[5] T. Inoue, J. Kamimae, M. Ueda, K. Eguchi and H. Arai, *J. Mater. Chem.* **3** (1993) 751.
[6] D. J. Vischjager, P. J. van der Put and J. Schonmann, *Solid State Ionics* **27** (1988) 199.
[7] Ch. Ftikos, S. Carter and B. C. H. Steele, *J. Euro. Ceram. Soc.* **12** (1993) 79.
[8] I. Riess, *Solid State Ionics* **44** (1991) 207.
[9] I. Riess, S. Kramer and H. L. Tuller, *in* 'Solid State Ionics' (edited by M. Balkanski, T. Takahashi and H. L. Tuller), Elsevier Science (1992) p. 499.
[10] M. V. Patrakeev, I. A. Leonidov, V. L. Kozhevnikov, V. I. Tsidilkovskii, A. K. Demin and VV. Nikolaev, *Solid State Ionics* **66** (1993) 61.
[11] C. Wagner, *Pro. Sol. State Chem.* **10** (1975) 3.
[12] H. J. M. Bouwmeester, H. Kruidhof, A. J. Burggraaf and P. J. Gellings, *Solid State Ionics* **53/56** (1992) 460.
[13] C. S. Chen, 'Fine Grained Zirconia-Metal Dual Phase Composites', PhD thesis, University of Twente (1994).
[14] Y. Teraoka, T. Nabunaga and N. Yamazoe, *Chem. Lett.* (1988) 503.
[15] T. Ishigaki, S. Yamauchi, J. Mizusaki and K. Fueki, *J. Solid State Chem.* **54** (1984) 100.
[16] O. Yamamoto, Y. Taketa, R. Kanno and M. Noda, *Solid State Ionics* **22** (1987) 241.
[17] J. Mizusaki, Y. Mima, S. Yamauchi and K. Fueki, *J. Solid State Chem.* **80** (1989) 102.
[18] M. Seppänen, M. Kyto and P. Taskinen, *J. Metall.* **9** (1980) 3.
[19] V. G. Bhide, D. S. Rajoria, G. Rama Rao, G. V. Subbarao and C. N. R. Rao, *Phys. Rev. Lett.* **28** (1972) 1133.
[20] K. Gaur, S. C. Verma and H. B. Lal, *J. Mater. Sci.* **23** (1988) 1725.